analytical chemistry

Article

pubs.acs.org/ac

Toward More Efficient Bioelectrocatalytic Oxidation of Ethanol for Amperometric Sensing and Biofuel Cell Technology

Barbara Kowalewska* and Pawel J. Kulesza*

Department of Chemistry, University of Warsaw, Pasteura 1, PL-02-093 Warsaw, Poland

Supporting Information

ABSTRACT: The integrated, structured, and multifunctional bioelectrocatalytic system for effective oxidation of ethanol is developed here. The concept is based on the layer-by-layer (LbL) assembly through electrostatic attraction of positively charged, multiwalled carbon nanotubes and the controlled combination of dehydrogenase enzymes. More specifically, the LbL technique was employed for sequential immobilization of two dehydrogenase enzymes and poly(diallyldimethylammonium chloride)-covered multiwalled carbon nanotubes onto a glassy carbon electrode substrate. Both monoenzymatic [utilizing a single enzyme, alcohol dehydrogenase (ADH)] and bienzymatic (anchoring sequentially both ADH and aldehyde dehydrogenase) systems were tested. Multilayers were characterized using scanning electron microscopy, infrared spectroscopy, and cyclic voltammetry. The results are consistent with the view that our approach enables good control of distribution and efficient utilization of both enzymes within the biocomposite film and leads to sizable enhancement of the oxidation of ethanol through significant (more than 2-fold) increase of bioelectrocatalytic currents and by shifting the ethanol oxidation potential to 0.1 V (vs Ag/AgCl) or decreasing the overvoltage by ca. 200 mV in comparison with the monoenzymatic electrode system. This simple biocomposite (enzyme-cascade) system permits fabrication of highly sensitive ethanol biosensors based on nicotinamide adenine dinucleotide coenzyme-dependent dehydrogenases. Our ethanol biosensor exhibited a good linearity ranging from 50 to 300 μM, and it was characterized by a high sensitivity of 118.8 μA mM^{-1} cm^{-2} as well as a low detection limit of 24 μM.

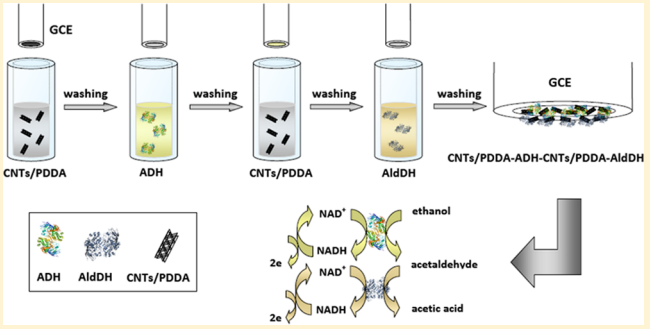

There has been growing interest in developing new bioelectrocatalytic-modified electrodes that exhibit a high stability, selectivity, and specificity during electrooxidation of ethanol. Although ethanol is as yet not commonly considered a fuel for use in electrochemical biofuel cells, it has some advantages related to its low cost and toxicity and its wide availability. Ethanol is considered a renewable biofuel because it can be produced through fermentation of agricultural products.[1,2] There is also a need to develop alternate analytical, including electroanalytical, concepts for simple, fast, and reliable determination of ethanol. Two kinds of enzymes, namely alcohol dehydrogenase (ADH), that is either pyrroloquinoline quinine (PQQ)-dependent[3−5] or nicotinamide adenine dinucleotide (NAD)-dependent,[6−20] and alcohol oxidase (AOx)[21−24] are typically considered biocatalysts for the construction of the amperometric ethanol biosensors. While the NAD-dependent ADH-based ethanol biosensors have the advantage of utilizing a more stable (relative to AOx and PQQ-ADH) biocomponent,[25] they suffer from the necessity of introducing the NAD^+ cofactor either by its addition to the supporting electrolyte or by immobilization on the electrode surface. The major disadvantage of the latter concept concerns possible leachability problems and poor operational stability of a biosensor. On fundamental electrochemical grounds, reoxidation of the NADH cofactor proceeds at bare electrode substrates at high overpotentials (ca. 1 V); consequently, many other reactants (e.g., existing in food samples) may interfere during the experiments.[8] The large overvoltage for NADH oxidation to NAD^+ is due to the rapid formation of dimers and accumulation of products on the electrode surface.[18,26]

To minimize the electrode surface fouling problem, several redox mediators[7−9] were considered to significantly decrease overpotential for the NADH oxidation. Sizeable improvement was also noticed when carbon nanotubes were utilized with[10−14] or without[15−20] redox mediators for fabrication of the ADH-based ethanol biosensors. Obviously carbon nanotubes (CNTs) tend to promote unimpeded distribution of charge at the bioelectrocatalytic interface, and their presence facilitates fast electron transfers between the immobilized enzyme and the electrode surface.

Recently, the ability of poly(diallyldimethylammonium chloride) (PDDA) to modify, solubilize, and functionalize CNTs has been demonstrated. The concept provides a useful way for preparing the CNT-binder composite-modified electrode transducer for a wide range of sensing applications.

Received: August 22, 2012
Accepted: October 15, 2012
Published: October 15, 2012

PDDA is a water-soluble quaternary ammonium cationic polyelectrolyte that exhibits good adhesion and film-forming capabilities. Consequently, distribution and dispersibility of PDDA-modified or stabilized CNTs can be improved in various (including aqueous) media. Practical examples include various functionalized CNT-based electronically conducting[16,27,28] and electrocatalytic[29] films. It is reasonable to hypothesize that in the presence of positively charged PDDA-modified CNTs, formation of the previously mentioned NAD^+-based dimers and/or accumulation of the products would be largely diminished at the bioelectrocatalytic interface.

The layer-by-layer (LbL) approach that utilizes CNTs and a PDDA modifier has successfully been adopted to prepare various enzyme configurations for biosensor applications.[30−32] The electrostatic attraction between the positively charged PDDA molecules and the negatively charged enzymes leads to the formation of stable and useful multiple biocomposites on the electrode surface. The main advantage of fabrication of multilayer systems concerns the ability to increase the biocomponents (recognition elements, biocatalytic centers) in a defined and systematic manner on electrode surfaces to achieve higher sensitivity and selectivity.

In the present work, fabrication and utilization of a novel biosensing/bioelectrocatalytic electrode for the oxidation of ethanol is described. Our concept of integration of biocatalytic components refers to our earlier studies on a CNT-supported single enzyme (e.g., ADH) system[33], but this time it aims at fabrication of a biocomposite system through controlled immobilization (using the electrostatic LbL technique) of two specific dehydrogenase enzymes [ADH and aldehyde dehydrogenase (AldDH)]. The system's bifunctional activity (oxidation of ethanol to acetaldehyde at ADH followed by rapid oxidation to acetic acid at AldDH) is facilitated by proper coupling of the enzymes' structures or "wiring" their reactive centers via PDDA-functionalized CNTs. Our study parallels existing concepts of formation of various cascade-type enzymatic systems[34] as well as the very recent approaches based on the two-step oxidation of ethanol to acetate using NAD^+-dependent enzymes, ADH, and AldDH for preparation of bioanodes for biofuel cells.[2,35] To comment on the formation, morphology, and physicochemical (including electroanalytical) properties of the resulting multilayer films, cyclic voltammetry, field emission scanning electron microscopy (FESEM), and FTIR have been used. Comparative bioelectrocatalytic measurements, involving both bienzymatic multilayered electrodes and monoenzymatic systems, are also described. This research is of importance to the development of amperometric ethanol biosensors and electrocatalytic materials for ethanol biofuel cells.

EXPERIMENTAL SECTION

Reagents and Materials. Alcohol dehydrogenase (ADH, EC 1.1.3.4, 400 units mg^{-1}) from Bakers Yeast (*Saccharomyces cerevisiae*), aldehyde dehydrogenase (AldDH, EC 1.2.1.3, 2 units mg^{-1}), β-nicotinamide adenine dinucleotide hydrate (NAD^+, from yeast), and acetaldehyde (≥99.5%) were obtained from Sigma. PDDA (of low molecular weight, 20 wt % in water), multiwalled CNTs (>99%, 6−13 nm o.d., 2.5−20 nm length) and Nafion (5 wt % solution of lower aliphatic alcohols and 15−20% water) were obtained from Aldrich. Ethanol (99.8%), methanol (32.04 g/mol), and 2-propanol (99.7%) were obtained from POCh. Alcohol stock solutions were stored at 4 °C. The phosphate buffer solution contained KH_2PO_4 and K_2HPO_4 (POCh). All chemicals were of analytical grade purity, and they were used as received.

Solutions were prepared just before their use from triply distilled subsequently deionized (Millipore Milli-Q) water. They were deaerated (using prepurified argon) for at least 15 min prior to the electrochemical experiment. Argon was used to deaerate solutions and to keep an air-free atmosphere over the solution during the measurements. Experiments were conducted at room temperature (25 ± 0.5 °C).

Apparatus and Methods. Electrochemical measurements were conducted with CH Instruments model 660B workstation (Austin, TX). All experiments were carried out with a conventional three-electrode system: the modified glassy carbon electrode (geometric area, 0.071 cm^2) as the working electrode, a platinum wire as the counter electrode, and a Ag/AgCl (saturated KCl) electrode as the reference electrode. Before modification, the glassy carbon electrode was first carefully activated with alumina on a polishing cloth.

Field emission scanning electron microscopy (FESEM) images were obtained using Zeiss (Merlin). Fourier transform infrared (FTIR) spectra were recorded using the infrared microscope, NICOLET iN10 MX (Thermo Scientific). The beam incidence angle was equal to 80° with respect to the surface normal. Typically 1000 scans were averaged for a single reflectance spectrum. The samples were deposited onto the glassy carbon plate followed by drying in air.

Preparation and Electrode Modification with PDDA-modified CNTs. To produce PDDA-modified carbon nanotubes, the respective suspension was formed by dispersing ca. 10 mg of CNTs (0.1−10 μm in length, 10−15 nm o.d., 2−6 nm i.d.) in 5 mL PDDA aqueous solution. The suspension was sonicated for 30 min and then mixed with a magnetic stirrer at ambient temperature for 12 h. Subsequently, it was centrifuged for 1 h, and the supernatant solution was removed and replaced with water and mixed. The procedures of washing out and centrifuging were done with water and repeated at least three times to remove the loosely adsorbed PDDA. Thus, a stable colloidal solution of PDDA-stabilized nanostructured carbon was obtained.

The film of PDDA-modified CNTs (CNTs/PDDA) was fabricated by immersing the glassy carbon electrode in the respective colloidal CNT suspension for 30 min. After that, it was thoroughly rinsed with water and allowed to dry at room temperature for about 30 min.

Fabrication of Multilayer Ethanol Biosensor. To prepare a single enzyme bioelectrocatalytic film, 1 mg ADH was dissolved in 0.25 mL 0.1 M phosphate buffer (pH = 8.0) and thoroughly mixed using a magnetic stirrer. Then, the CNTs/PDDA-modified glassy carbon electrode was immersed in the enzyme solution for 30 min. This step was followed by rinsing with phosphate buffer (pH = 8.0) and drying in ambient temperature. In order to prevent the leakage of enzyme molecules from the surface, the electrode was dipped into a 0.5% aqueous Nafion solution. The resulting layer was allowed to dry for 1 h at room temperature. Following the preparation, the electrode was rinsed 3−4 times by dipping it in phosphate buffer (pH = 8.0). When not in use, the electrode was kept in a 0.1 M phosphate buffer (pH = 8.0) at 4 °C in a refrigerator.

To obtain a bilayer (bienzymatic cascade-type) system, the electrode with CNTs/PDDA−ADH was immersed, before dipping it in the Nafion solution, in a colloidal suspension of PDDA-modified CNTs and then in a solution of the respective enzyme, ADH or AldDH (1 mg in 0.25 mL 0.1 M phosphate

dx.doi.org/10.1021/ac3021328 | Anal. Chem. 2012, 84, 9564−9571

buffer at pH = 8.0). To produce multilayer films, the concept of electrostatic attraction between positively charged PDDA-modified CNTs and negatively charged enzyme molecules was further explored, and all additional steps of immersing the glassy carbon electrode were repeated in the appropriate sequence.

Prior to the bioelectrocatalytic diagnostic experiments, the electrode was conditioned by voltammetric potential cycling between −0.1 and 0.7 V in 0.1 M phosphate buffer (pH = 8.0) for ca. 20 min.

RESULTS AND DISCUSSION

Cyclic Voltammetric Characterization of Multilayered ADH with PDDA-Modified CNTs. Figure 1 A (curves a−d)

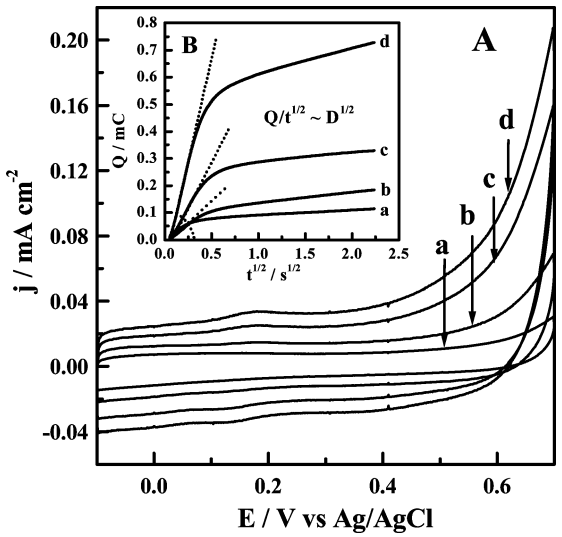

Figure 1. (A) Cyclic voltammograms recorded for the following multilayered films: (a) $(CNTs/PDDA\text{-}ADH)_1$, (b) $(CNTs/PDDA\text{-}ADH)_2$, (c) $(CNTs/PDDA\text{-}ADH)_3$, and (d) $(CNTs/PDDA\text{-}ADH)_4$ deposited on glassy carbon. The number of layers are provided in subscripts. Inset (B) illustrates the respective chronocoulometric responses of charge (Q) plotted vs square root of time ($t^{1/2}$) recorded upon application of the potential step from −0.1 to 0.7 V. Electrolyte: deoxygenated 0.1 M phosphate buffer at pH = 8.0. Scan rate: 5 mV s^{-1}. Pulse width: 5 s.

illustrates typical voltammetric responses of the multilayer films of the type $(CNTs/PDDA\text{-}ADH)_n$, where n = 1−4, recorded in deaerated 0.1 M phosphate buffer solution (PBS, pH = 8.0) as a supporting electrolyte. Some residual peaks (not clearly defined) at about 0.1−0.2 V shall be attributed to the well-known the redox behavior of the oxygen-containing groups on the walls of CNTs.[31,36,37] Growing currents appearing at potentials higher than 0.6 V should be attributed to the oxidation of PDDA. Following assembling the multilayer film via consecutive LbL steps, the observed current densities increased uniformly thus indicating the uniform growth of CNTs/PDDA-ADH layers at the electrode. These results also imply effective immobilization of ADH on PDDA-modified CNTs by using LbL technique. For all films considered, virtually no changes in the voltammetric characteristics of the respective responses have been observed during repetitive electrochemical experiments performed within a period of at least a week. This result is consistent high electrochemical stability of biocatalytic films.

Dynamics of Charge Transport in Multilayer Film. It has been commonly accepted that effective mediating systems for bioelectrocatalysis must be capable of fast distribution of electrons to the enzyme sites. In other words, in addition to specific reactivity, dynamics of charge transport in bioelectrocatalytic films must be fast. Here our multilayer films (as for Figure 1 A) were diagnosed using a single potential oxidative step (from −0.1 to 0.7 V) chronocoulometry. Curves a−d in Figure 1 B illustrate dependencies (recorded in deaerated phosphate buffer solution at pH = 8.0) of the chronocoulometric charge, Q accumulating during the reduction of the assembled $(CNTs/PDDA\text{-}ADH)_n$ (n = 1−4) films on the square root of time, $t^{1/2}$. Such plots can be diagnosed[38] to distinguish between two regions where charge propagation can be described in terms of either semi-infinite diffusion or thin layerlike behavior. It comes from the shapes of the plots in Figure 1 B that these two distinct patterns can be correlated to two time domains: application of shorter (t < 0.25 s) and longer (t > 0.25 s) pulses. For longer potential steps applied, the thin-layer limit becomes operative, and the dependency of Q on $t^{1/2}$ reaches a plateau due to practically complete oxidative electrolysis of the film. But linear portions of the chronocoulometric plots (Figure 1 B) that appear where the diffusion layer thickness, $[2D_{eff}t]^{1/2}$, is much smaller than the film thickness, d, can effectively be approximated in diffusion-like terms, namely with the use of an effective diffusion (transport) coefficient, D_{eff}. Under such conditions, the dependence of Q on $t^{1/2}$ is expressed with the integrated Cottrell equation

$$[Q/t^{1/2}] = 2nF\pi^{1/2}r^2[D_{eff}{}^{1/2}C_o] \quad (1)$$

where r and C_o stand for the radius and concentration of redox centers, respectively, whereas other parameters have their usual significance.[38] From the linear portion of the dependence of Q on $t^{1/2}$, one can determine the slope, $[Q/t^{1/2}]$, and indirectly, the charge transport dynamics parameter, $[D_{app}{}^{1/2}C_o]$. Since it is difficult to determine precisely the C_o values, comparisons of the $[D_{app}{}^{1/2}C_o]$ parameters, rather than more roughly estimated D_{app}'s, are more justified here. The slopes of curves a, b, c, and d increase as follows: 0.26, 0.27, 0.58, and 1.32 mC s$^{-1/2}$ thus indicating that the charge propagation becomes faster in multilayer $(CNTs/PDDA\text{-}ADH)_n$ films, at least up to n = 4. Consequently, values of the $[D_{app}{}^{1/2}C_o]$ charge transport parameters increase from 3.4 × 10^{-8} mol cm^{-2} s$^{-1/2}$ (Figure 1 B, curve a) to 1.7 × 10^{-7} mol cm^{-2} s$^{-1/2}$ (Figure 1 B, curve d). When compared to typical $[D_{app}{}^{1/2}C_o]$ values ranging from 0.2 to 1.0 × 10^{-7} mol cm^{-2} s$^{-1/2}$ that are characteristic of model systems involving one-electron transfers (e.g., in well-behaved redox polymer films on electrodes characterized by D_{app}'s and C_o's on the level from 10^{-10} to 10^{-8} cm^2 s^{-1} and from 0.2 to 1.0 mM cm^{-3}, respectively), the values obtained in the present work are consistent with the view that the overall dynamics of charge transport in the multilayer $(CNTs/PDDA\text{-}ADH)_n$ films are fairly high. The fact that the "linear" portions of chronocoulometric curves (Figure 1 B) tended to produce neither positive deviations from linearity nor sizable negative intercepts[39] supports our view about the absence of significant ohmic and kinetic limitations to charge transport within the investigated multilayer films.

Morphology of Multilayer Systems. Three different films, CNTs/PDDA, $(CNTs/PDDA\text{-}ADH)_1$, and $(CNTs/PDDA\text{-}ADH)_2$ have been prepared on glassy carbon plates in a manner analogous to that described in Experimental Section for modification of regular disk electrodes. The homogeneity of

dx.doi.org/10.1021/ac3021328 | Anal. Chem. 2012, 84, 9564−9571

the deposited films were characterized using FESEM. A comparison of the images (a), (b), and (c) in Figure 2 shows

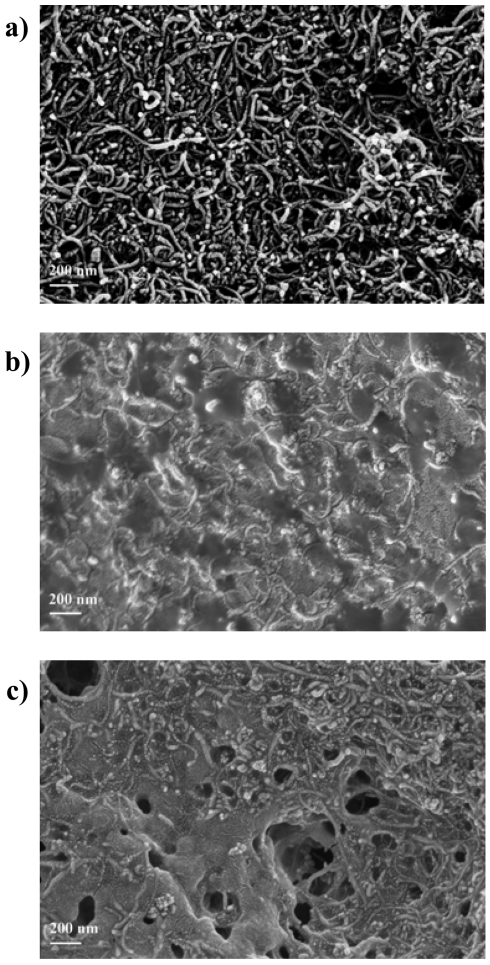

Figure 2. Scanning electron microscope images of glassy carbon surfaces modified with (a) CNTs/PDDA, (b) $(CNTs/PDDA\text{-}ADH)_1$, and (c) $(CNTs/PDDA\text{-}ADH)_2$.

significant morphological differences between those films. While simple deposits of PDDA-modified CNTs (Figure 2 a) are characterized by a fairly uniform but rather loose distribution of components, the multilayer biocomposite films (Figure 2, panels b and c) exhibit much denser morphologies. This observation is particularly true for thicker multilayered structures on electrodes (Figure 2 c). It is reasonable to expect that positively charged CNTs/PDDA "nanowires" attract anionic sites of ADH-enzyme domains.

Physicochemical Identity of ADH-Containing Multilayer Films. The following systems, enzyme-free CNTs/PDDA as well as enzyme-containing $(CNTs/PDDA\text{-}ADH)_1$ and $(CNTs/PDDA\text{-}ADH)_2$, were deposited on a glassy carbon plate and characterized by monitoring FTIR reflectance absorption spectra (Figure S1 of the Supporting Information). It is not surprising that the spectrum of CNTs/PDDA (Figure S1 A, curve a of the Supporting Information) shows a well-defined peak at 2937 cm^{-1} typically attributed to the stretching vibration bands of $-CH_2$ and $-CH_3$ groups existing in a PDDA molecule. Further, the vibration band of the PDDA cycle appears at 1469 cm^{-1}. All these findings are consistent with earlier results.[16,40]

Colloidal suspensions of CNTs/PDDA show remarkable stability without any observable flocculations or aggregations for at least 6 months, thus suggesting that PDDA acts as an effective protecting agent for CNTs. Uniform dispersion of CNTs/PDDA nanostructures is facilitated by the existence of electrostatic repulsion forces while using PDDA as a protecting agent for gold or silver nanoparticles.[40,41] As postulated earlier for polyoxometalate or tetrathiafulvalene adsorbates on partially polymerized layers of 4-(pyrrole-1-yl) benzoic acid on CNTs, PDDA is likely to undergo strong adsorption not only at defective places of sidewalls but also at both ends of CNTs.[42−44]

We have also recorded the FTIR spectrum of a bioelectrocatalytic film of CNTs/PDDA overcoated with the ADH enzyme (Figure S1 A, curve b of the Supporting Information). IR spectrum of the immobilized enzyme provides information about its secondary structure and evidence about retaining the native form of a protein upon immobilization. The vibration bands appearing in Figure S1 A, curve b of the Supporting Information at 1656 cm^{-1} (amide I) and 1543 cm^{-1} (amide II), which are typical for the ADH enzyme, originate from the C═O (carbonyl) stretching vibration of peptide linkages and from the combination of the N−H in-plane bending with the C−N stretching vibration of the peptide groups of ADH, respectively. The fact that only small shifts in the positions of amide I and amide II vibration bands have been observed following introduction of the enzyme onto CNTs/PDDA (Figure S1 B, curves b and c of the Supporting Information) implies no denaturation of the protein as well as no conformation changes in the enzyme's original secondary structure[16,33,45] upon immobilization.

Biolectrocatalytic Oxidation of Ethanol at the Multilayer Film. We have addressed voltammetric oxidation of ethanol (Figure 3 A, curves a−d) at $(CNTs/PDDA\text{-}ADH)_n$, multilayer films (where n = 1−4) recorded in neutral medium (0.1 M phosphate buffer at pH = 8.0 containing 5 mM NAD^+).

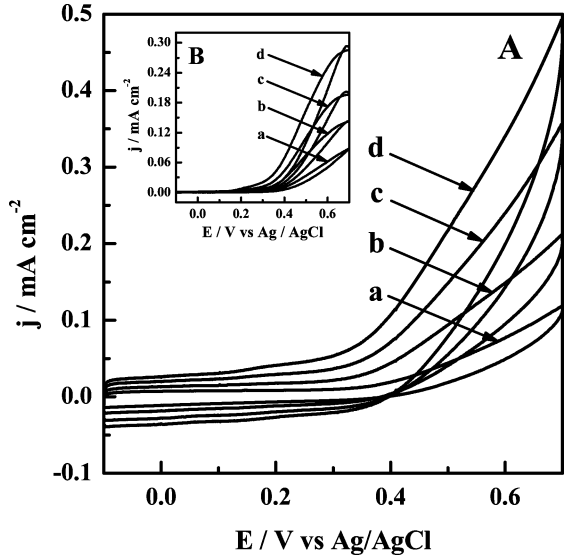

Figure 3. Voltammetric oxidation of ethanol at the glassy carbon electrode covered with the following films: (a) $(CNTs/PDDA\text{-}ADH)_1$, (b) $(CNTs/PDDA\text{-}ADH)_2$, (c) $(CNTs/PDDA\text{-}ADH)_3$, (d) $(CNTs/PDDA\text{-}ADH)_4$ (A) before and (B) after background subtraction. Electrolyte: deoxygenated 0.1 M phosphate buffer at pH = 8.0 containing 20 mM ethanol and 5 mM NAD^+. Scan rate: 5 mV s^{-1}.

dx.doi.org/10.1021/ac3021328 | Anal. Chem. 2012, 84, 9564−9571

Although oxidation of ethanol does not proceed at impressively low potentials, as expected for the powerful bioelectrocatalytic system, an important observation coming from the data of Figure 3 (particularly from the background subtracted curves of Figure 3 B showing "net" electrooxidation currents) is that the electrocatalytic currents increase (whereas the oxidation overpotential tends to decrease) with growing thickness of the film, namely loading of PDDA-modified CNTs and the supported ADH enzyme. The results are consistent with the view that the enzyme can be successfully utilized even at thicker films. Further, they are in agreement with our findings concerning fast dynamics of charge propagation and dense morphology (large population of active sites) of multilayer films. Among other important issues is availability and uniform distribution of CNTs that facilitate fast distribution of electrons to the enzyme active sites. The importance of full coverage by CNTs was already emphasized for self-assembled polyelectrolyte multilayers.[46]

As demonstrated earlier[33] that neither PDDA-modified CNTs nor bare CNTs with an ADH enzyme show separately appreciable catalytic reactivity toward ethanol oxidation in 0.1 M phosphate buffer (pH = 8.0). Electron transfers from active sites of ADH to the electrode surface are obviously facilitated by the presence of CNTs, but the presence of PDDA makes the later process more efficient, though, the exact nature of improved "wiring" of the enzyme to the electrode surface is still unclear.

To optimize conditions of the bioelectrocatalytic experiment, we performed a series of measurements aimed at determining the dependence of electrocatalytic responses of electrodes on the solution pH and the concentration of NAD^+ (for simplicity the results are not shown here). We found that maximum sensitivity was achieved at pH = 8.0 with the concentration of NAD^+ equal to 5 mM. The optimum pH for the enzyme activity is obviously dependent on the immobilization method and local microenvironment.

Catalytic Reactivity of Biocomposite Film Utilizing Layer-By-Layer ADH and AldDH. The multilayer films containing two dehydrogenase enzymes, ADH and AldDH, have been found to show the best electrocatalytic performance in terms of the lowest ethanol oxidation potential and the highest oxidation current densities. It was established earlier[34] that when the enzymes are properly coupled (i.e., deposited in a proper sequence and wired), the activity of the biocomposite film should be enhanced due to the possibility of an increase in the number of electrons exchanged by the system. It is apparent from the data of Figure 4 that, indeed, current densities for the oxidation of ethanol are the highest at the bienzymatic system, and the reaction is shifted toward less positive values when both ADH and AldDH are employed.

When referring to fundamentals of electrochemistry,[38,47] the overall electrocatalytic process utilizing two enzymes (biocatalysts) can be approximated in terms of either (1) an electrode reaction (electrooxidation of ethanol to acetaldehyde at ADH) followed by a chemical reaction (biocatalytic oxidation of acetaldehyde to acetic acid at electrochemically-activated AldDH existing within three-dimensional solution-like film) or (2) a simple reaction with two steps in which the product of the first electron-transfer reaction undergoes a second electron-transfer step. In the latter situation, a multielectron overall response arises only when the second electron-transfer reaction is thermodynamically more favorable (for oxidations appearing at less positive potentials) than the first one.[38] It is apparent upon comparison of Figures 3 and 4, that oxidation of acetaldehyde starts at the film utilizing both ADH and AldDH enzymes at almost 200 mV less positive potential (Figure 4 A) when compared to the behavior of ethanol at the film containing the ADH enzyme only (Figure 3). The concept based on the following reaction emphasizes the importance of the dynamics of the second step.[47] Under voltammetric conditions for oxidation processes, the peak potential (E_p) is expected to be shifted with respect to the expected half-wave potential ($E_{1/2}$) in the following manner[38,47]

$$E_p = E_{1/2} + (RT/nF)0.780 - (RT/2nF)\ln(RT/nF) - (RT/2nF)\ln k/v \quad (2)$$

where k is the rate constant for the pseudo-first-order reaction (here it can serve as a kinetic parameter for the approximate description of the second step), and v stands for scan rate. It

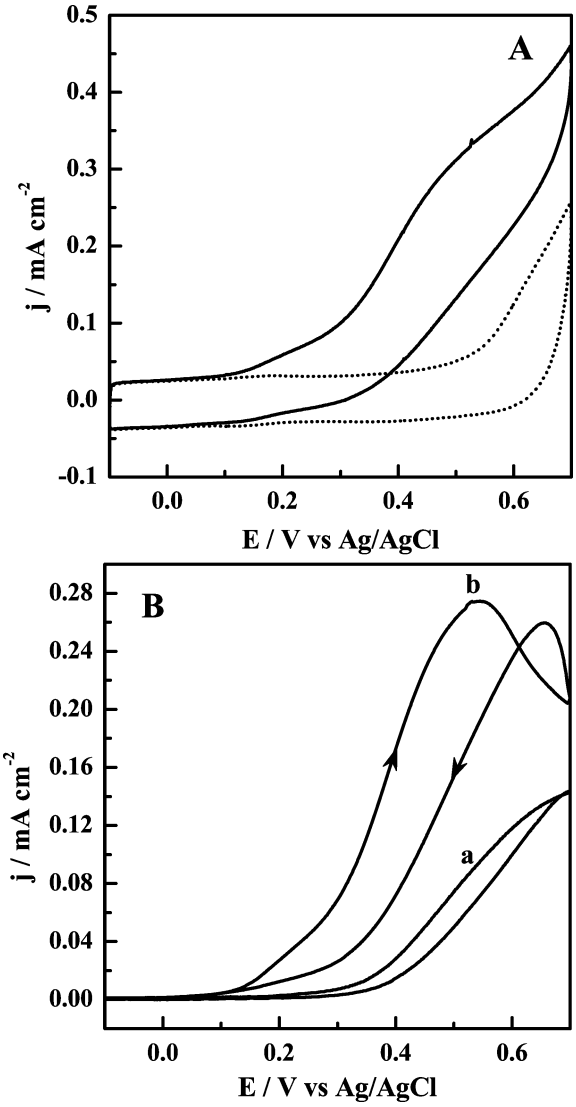

Figure 4. (A) Cyclic voltammetric responses recorded at the glassy carbon electrode covered with biocomposite CNTs/PDDA-ADH–CNTs/PDDA-AldDH film in the presence (solid line) and absence (dotted line) of 20 mM ethanol. (B) Background subtracted voltammograms are provided for the following films: (a) $(CNTs/PDDA\text{-}ADH)_2$ and (b) CNTs/PDDA-ADH–CNTs/PDDA-AldDH. Other conditions are the same as those given for Figure 3.

dx.doi.org/10.1021/ac3021328 | Anal. Chem. 2012, 84, 9564–9571

can be rationalized based on eq 2 and the literature data[38,47] that, in the case of voltammetric oxidations executed at fairly low v values (up to 20 mV s^{-1}), the peak potential would shift more than 100 mV toward more negative values for the systems characterized by k values as high as 10^5–10^8 mol^{-1} dm^3 s^{-1}.

Figure 4 B illustrates background-subtracted cyclic voltammograms for the oxidation of ethanol at the single-enzyme bilayer $(CNTs/PDDA\text{-}ADH)_2$ film (curve a) and the biocomposite two-enzyme bilayer CNTs/PDDA-ADH–CNTs/PDDA-AldDH film (curve b), respectively. It is noteworthy that oxidation of ethanol starts at the biocomposite (containing ADH together with AldDH) film (Figure 4 B, curve b) at a quite low (0.1 V) potential (i.e., at the value certainly less positive when compared to the simple ADH-based film (Figure 4 B, curve a). The substantial negative shift (ca. 0.2 V) and the observed more than 2-fold larger peak current signal demonstrate that the ADH and AldDH enzymes have been successfully integrated (with the use of PDDA-modified CNTs) to significantly enhance the oxidation of ethanol. The overall process is expected to proceed according to the scheme

$$CH_3CH_2OH + NAD^+ \rightarrow CH_3CHO + NADH + H^+ \quad (3)$$

$$CH_3CHO + NAD^+ \rightarrow CH_3COOH + NADH + H^+ \quad (4)$$

where the NAD^+ cofactor existing in solution participates directly in the reaction mechanism and is regenerated at the electrode surface as follows

$$NADH - 2e - H^+ \rightarrow NAD^+ \quad (5)$$

Both oxidations (eqs 3 and 4) involve two electrons and their effective coupling translates into a situation where the total reaction becomes four electron in nature (i.e., the oxidation of ethanol proceeds to acetic acid as final product). This view is supported with observations summarized in Figure 5 clearly showing that the bioelectrocatalytic system utilizing AldDH enzyme is capable of effective oxidation of the acetaldehyde to acetic acid starting at potentials as low as 0.1 V. Such a reaction is not feasible at the simple ADH bioelectrocatalytic film. Combination of two enzymes may also induce a synergistic effect resulting in higher electrocatalytic currents than one would expect from the simple increase of a number of electrons transferred from 2 to 4. A comparison of peak currents in curves a and b (Figure 4 B) is consistent with this view. Finally, the fact that the positive (oxidation) currents have also been observed during the reverse negative potential scan (watch arrows in curve b) reflects the fact that oxidation of ethanol still proceeds because it has not been completed in the forward scan.

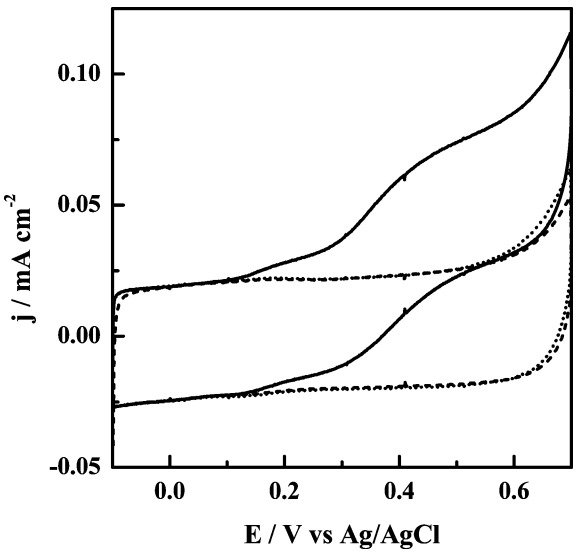

Figure 5. Voltammetric oxidation of 15 mM acetaldehyde (solid line) and 15 mM ethanol (dotted line) recorded at the bilayer CNTs/PDDA-AldDH–CNTs/PDDA-AldDH film in a 0.1 M phosphate buffer (pH = 8.0) containing 5 mM NAD^+. Other conditions as for Figure 3.

Comparison of the present results with earlier reports dealing the ethanol oxidation at such systems as chitosan modified carbon nanotubes[18] or simple ADH based films[33] clearly implies that the bienzymatic biocomposite film drives oxidation potential at truly low potentials. When compared to carbon natotube-ionic liquid and chloropromazine modified electrode[13] the CNTs/PDDA-ADH–CNTs/PDDA-AldDH film has similar oxidation potential. Selectivity of response of the combine ADH/AldDH bioelectrode has also been evaluated by considering methanol and 2-propanol as potential interfering reactants. In a case of methanol virtually no current responses in the investigated range of potential are obtained. On the other hand, in the presence of 2-propanol, the current response was seven times smaller than that for ethanol.

Stability of the composite (bienzymatic) bioelectrocatalytic system was diagnosed by executing comparative cyclic voltammetric measurements (ethanol oxidations) on the series of independently prepared hybrid films composed of the enzyme and the PDDA-modified CNTs. The fact, that the catalytic currents were reproducible within 8%, and they did not decrease following long-term experimentation (at least for two weeks) in the presence of ethanol, implies overall physicochemical stability of the system, durability of its electrocatalytic activity, as well as permanence of the enzyme immobilization on its surface.

Potential applications both in amperometric biosensors and as anode in the alcohol biofuel cell technology would require development of stable current responses with time. Figure 6 illustrates the respective chronoamperograms recorded at 0.5 V for two systems: (a) single enzyme bilayer $(CNTs/PDDA\text{-}ADH)_2$, and (b) bienzymatic CNTs/PDDA-ADH–CNTs/PDDA-AldDH. The striking feature coming from the data of Figure 6 is that the latter system produces a stable and reproducible current–time response that is much more larger in comparison to the that characteristic of the system utilizing only the ADH enzyme.

Amperometric Biosensing of Ethanol. The good electrochemical performance of CNTs/PDDA-ADH–CNTs/PDDA-AldDH film toward oxidation of ethanol led us to construct a representative amperometric biosensor based on the substrates of NAD^+-dependent dehydrogenases. As an example, the ethanol biosensor based on ADH and AldDH enzymes and PDDA-modified CNTs was constructed. At the same time, we were able to verify whether, in a broad range of concentrations, the combination of two enzymes, ADH and AldDH, (adsorbed onto CNTs/PDDA) efficiently catalyzed (in the presence of cofactor NAD^+) the oxidation of ethanol in the two-step process involving rapid oxidative decomposition of an acetaldehyde intermediate. Figure 7 A illustrates the steady-state responses recorded amperometrically at 0.5 V in 0.1 M

dx.doi.org/10.1021/ac3021328 | Anal. Chem. 2012, 84, 9564–9571

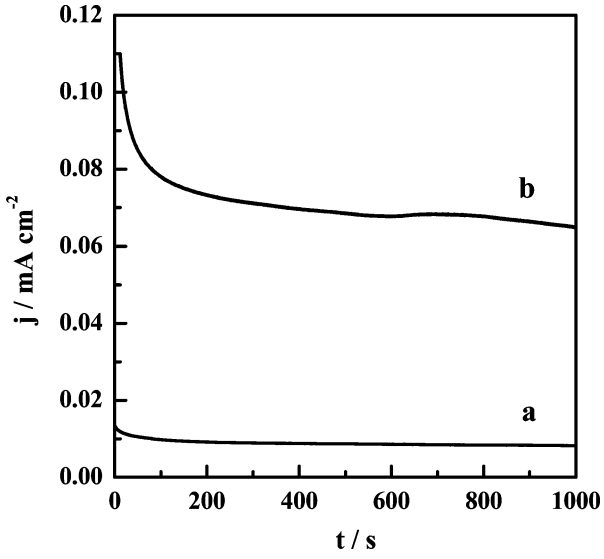

Figure 6. Chronoamperometric responses recorded at 0.5 V for the oxidation of 20 mM ethanol at (a) the bilayer $(CNTs/PDDA\text{-}ADH)_2$ and (b) biocomposite CNTs/PDDA-ADH−CNTs/PDDA-AldDH films. Other conditions are the same as those given for Figure 3.

PBS at pH = 8.0 upon systematically injecting ethanol in 0.05 mM steps. The response time did not exceed 5 s, so we can consider the sensor's response as fairly fast. The anodic current increased linearly with ethanol concentration over the range from 50 to 300 μM. The limit of detection was estimated at a signal-to-noise ratio of 3 to be 24 μM, which was much lower than those of 50 μM, 0.1 mM, and 90 μM reported earlier for biosensors utilizing alcohol dehydrogenase deposited on single-walled CNTs modified with poly(nile blue A),[11] poly(brilliant cresyl blue)[14], and PDDA,[16] respectively. The proposed ethanol biosensor also had good reproducibility. The relative standard deviation of the current response to 100 μM ethanol at 0.5 V was 3.1% for six successive measurements. When the ethanol concentration was high enough, a plateau current was observed showing the pattern characteristic of Michaelis−Menten kinetics (Figure 7 B). Using the electrochemical version of the Lineweaver−Burk equation, the apparent Michaelis−Menten (K_M^{app}) and sensitivity were calculated (Figure 7 C).[44] The value of K_M^{app} found for the bienzymatic bioelectrocatalytic system was on the level 0.33 mM. The value is definitely lower when compared to those typically reported in the literature.[11,16,19] The system's sensitivity of 118.8 μA mM^{-1} cm^{-2} is much higher[10,13,20] or similar[18] to the values obtained for biosensors reported earlier. These parameters indicate that the biocomposite film exhibits high bifunctional electrocatalytic activity toward oxidation of ethanol in a broad range of concentrations which makes it useful for sensor applications.

We have also addressed the performance of a CNTs/PDDA-ADH−CNTs/PDDA-AldDH-modified electrode following storage in the refrigerator at 4 °C. After one week and one month, the current responses were on the levels of 93% and 75%, respectively, of the initial values. These characteristics imply that bioactivities of dehydrogenase enzymes are retained under amperometric conditions and make the system useful for repetitive applications.

CONCLUSIONS

We demonstrate the usefulness of sequential and controlled coupling of two dehydrogenase enzymes, ADH and AldDH,

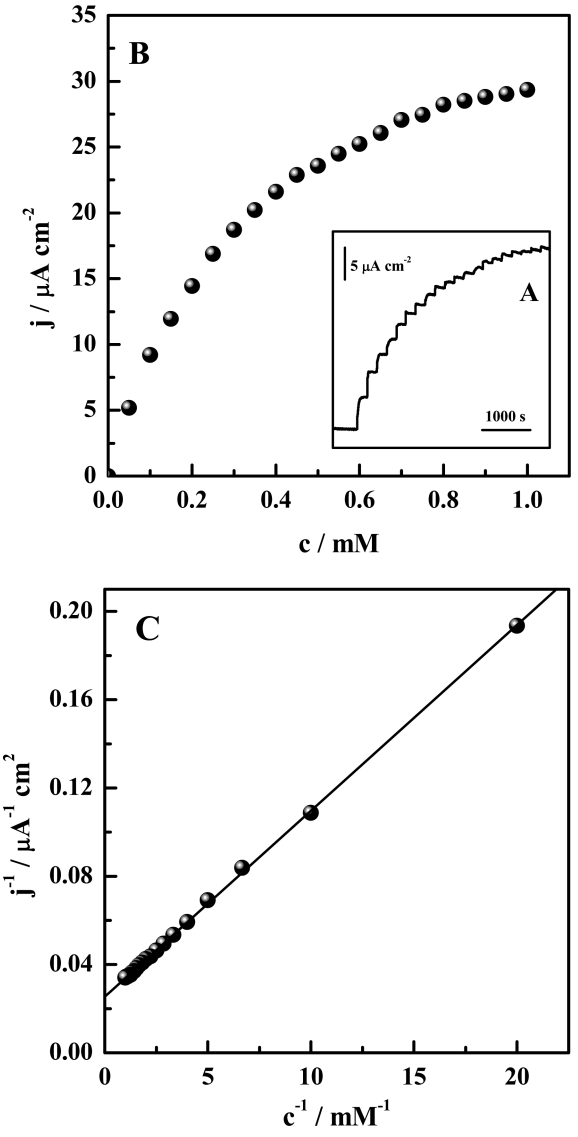

Figure 7. (A) Chronoamperometric current−time responses recorded upon application of 0.5 V at the CNTs/PDDA-ADH−CNTs/PDDA-AldDH film (deposited on a glassy carbon electrode) during successive additions of 0.05 mM ethanol. (B) Calibration curve obtained from the data of (A) as a function of ethanol concentration. (C) The Lineweaver−Burk plot. Electrolyte: deoxygenated 0.1 M phosphate buffer at pH = 8.0 containing 5 mM NAD^+.

together with the polyelectrolyte, namely poly(diallyldimethylammonium chloride)/PDDA, covered multiwalled carbon nanotubes (CNTs). Integration and stabilization of various components within the biocomposite electrocatalytic film is achieved through electrostatic attraction between positively charged CNTs/PDDA and negatively charged dehydrogenase enzymes in the PBS electrolyte at pH = 8.0. While CNTs improve the overall distribution of charge, properly deposited and utilized dehydrogenase enzymes produce a bifunctional bioelectrocatalytic interface capable of driving two reactions, namely the oxidation of the ethanol and acetaldehyde intermediate, simultaneously to effectively transfer four electrons and to produce acetic acid as a final product. Consequently, oxidation of ethanol at the CNTs/PDDA-ADH−CNTs/PDDA-AldDH biocomposite film is characterized by high sensitivity, fairly low potential ethanol detection,

dx.doi.org/10.1021/ac3021328 | Anal. Chem. 2012, 84, 9564−9571

good repeatability, and reproducibility with appreciable operational stability under the storage conditions. Thus the novel biosensor will provide a promising perspective for the development and fabrication NAD^+-dependent dehydrogenases biosensors, biofuel cells, and other bioelectrochemical devices.

■ ASSOCIATED CONTENT

Supporting Information

One figure, showing FTIR spectra described in the text. This material is available free of charge via the Internet at http://pubs.acs.org.

■ AUTHOR INFORMATION

Corresponding Author

*B.K.: e-mail: bstar@chem.uw.edu.pl; tel, +48-22-8220211 ext. 373; fax, +48-22-8225996. P.J.K.: e-mail, pkulesza@chem.uw.edu.pl; tel, +48-22-8220211 ext. 289; fax, +48-22-8225996.

Notes

The authors declare no competing financial interest.

■ ACKNOWLEDGMENTS

This work was supported by the National Centre for Research and Development (NCBR, Poland) under Project 120000-601/58-PBR and by the Foundation for Polish Science (FNP, Poland) through the Chair (*Mistrz*) Program. B.K. was supported in part by the University of Warsaw under the BST project for young investigators.

■ REFERENCES

(1) Ramanavicius, A.; Kausaite, A.; Ramanaviciene, A. *Biosens. Bioelectron.* **2008**, *24*, 761−766.
(2) Akers, N. L.; Moore, C. M.; Minteer, S. D. *Electrochim. Acta* **2005**, *50*, 2521−2525.
(3) Ramanavicius, A.; Kausaite, A.; Ramanaviciene, A. *Sens. Actuators, B* **2006**, *113*, 435−444.
(4) Laurinavicius, V.; Razumiene, J.; Kurtinaitiene, B.; Lapenaite, I.; Bachmatova, I.; Marcinkeviciene, L.; Meskys, R.; Ramanavicius, A. *Bioelectrochemistry* **2002**, *55*, 29−32.
(5) Niculescu, M.; Mieliauskiene, R.; Laurinavicius, V.; Csöregi, E. *Food Chem.* **2003**, *82*, 481−489.
(6) Lobo, M. J.; Miranda, A. J.; Tunon, P. *Electroanalysis* **1996**, *8*, 932−937.
(7) Sprules, S. D.; Hartley, I. C.; Wedge, R.; Hart, J. P.; Pittson, R. *Anal. Chim. Acta* **1996**, *329*, 215−221.
(8) Mullor, S. G.; Sanchez-Cabezudo, M.; Ordieres, A. J. M.; Ruiz, B. L. *Talanta* **1996**, *43*, 779−784.
(9) Dai, Z. H.; Liu, F. X.; Lu, G. F.; Bao, J. C. *J. Solid State Electrochem.* **2008**, *12*, 175−180.
(10) Santos, A. S.; Pereira, A. C.; Duran, N.; Kubota, L. T. *Electrochim. Acta* **2006**, *52*, 215−220.
(11) Du, P.; Liu, S. N.; Wu, P.; Cai, C. X. *Electrochim. Acta* **2007**, *53*, 1811−1823.
(12) Antiochia, R.; Lavagnini, I. *Anal. Lett.* **2006**, *39*, 1643−1655.
(13) Salimi, A.; Lasghari, S.; Noorbakhash, A. *Electroanalysis* **2010**, *22*, 1707−1716.
(14) Yang, D. W.; Liu, H. H. *Biosens. Bioelectron.* **2009**, *25*, 733−738.
(15) Rubianes, M. D.; Rivas, G. A. *Electroanalysis* **2005**, *17*, 73−78.
(16) Liu, S.; Cai, C. *J. Electroanal. Chem.* **2007**, *602*, 103−114.
(17) Tsai, Y. C.; Huang, J. D.; Chiu, C. C. *Biosens. Bioelectron.* **2007**, *22*, 3051−6.
(18) Lee, C. A.; Tsai, Y. C. *Sens. Actuators, B* **2009**, *138*, 518−523.
(19) Manso, J.; Mena, M. L.; Yanez-Sedeno, P.; Pingarron, J. M. *Electrochim. Acta* **2008**, *53*, 4007−4012.
(20) Yuan, J. H.; Chen, J. R.; Wu, X. H.; Fang, K. M.; Niu, L. *J. Electroanal. Chem.* **2011**, *656*, 120−124.
(21) Vijayakumar, A. R.; Csöregi, E.; Heller, A.; Gorton, L. *Anal. Chim. Acta* **1996**, *327*, 223−234.
(22) Gouveia-Caridade, C.; Pauliukaite, R.; Brett, C. M. A. *Electrochim. Acta* **2008**, *53*, 6732−6739.
(23) Barsan, M. M.; Brett, C. M. A. *Talanta* **2008**, *74*, 1505−1510.
(24) Smutok, O.; Ngounou, B.; Pavlishko, H.; Gayda, G.; Gonchar, M.; Schuhmann, W. *Sens. Actuator, B* **2006**, *113*, 590−598.
(25) Tkac, J.; Vostiar, I.; Gemeiner, P.; Sturdik, E. *Bioelectrochemistry* **2002**, *56*, 127−129.
(26) Bartlett, P. N.; Simon, E.; Toh, C. S. *Bioelectrochemistry* **2002**, *56*, 117−122.
(27) Rouse, J. H.; Lillehei, P. T. *Nano Lett.* **2003**, *3*, 59−62.
(28) Kim, B.; Park, H.; Sigmund, W. M. *Langmuir* **2003**, *19*, 2525−2527.
(29) Wang, D. L.; Lu, S. F.; Kulesza, P. J.; Li, C. M.; De Marco, R.; Jiang, S. P. *Phys. Chem. Chem. Phys.* **2011**, *13*, 4400−4410.
(30) Zhao, H.; Ju, H. *Anal. Biochem.* **2006**, *350*, 138−144.
(31) Zhang, J.; Feng, M.; Tachikawa, H. *Biosens. Bioelectron.* **2007**, *22*, 3036−3041.
(32) Eguilaz, M.; Villalonga, R.; Yanez-Sedeno, P.; Pingarron, J. M. *Anal. Chem.* **2011**, *83*, 7807−7814.
(33) Kowalewska, B.; Kulesza, P. J. *Electroanalysis* **2012**, *24*, 254−263.
(34) Sokic-Lazic, D.; Arechederra, R. L.; Treu, B. L.; Minteer, S. D. *Electroanalysis* **2010**, *22*, 757−764.
(35) Neto, S. A.; Forti, J. C.; Zucolotto, V.; Ciancaglini, P.; de Andrade, A. R. *Biosens. Bioelectron.* **2011**, *26*, 2922−2926.
(36) Wang, J.; Li, M.; Shi, Z.; Li, N.; Gu, Z. *Anal. Chem.* **2002**, *74*, 1993−1997.
(37) Luo, H.; Shi, Z.; Li, N.; Gu, Z.; Zhuang, Q. *Anal. Chem.* **2001**, *73*, 915−920.
(38) Bard, A. J.; Faulkner, L. R. *Electrochemical Methods*, 2nd ed.; Wiley: New York, 2001.
(39) Kulesza, P. J.; Malik, M. A.; Wieckowski, A. *Interfacial Electrochemistry*; Marcel Dekker: New York, 1999.
(40) Chen, H.; Wang, Y.; Wang, Y.; Dong, S.; Wang, E. *Polymer* **2006**, *47*, 763−766.
(41) Mayer, A. B. R.; Hausner, S. H.; Mark, J. E. *Polym. J. (Tokyo, Japan)* **2000**, *32*, 15−22.
(42) Kulesza, P. J.; Skunik, M.; Baranowska, B.; Miecznikowski, K.; Chojak, M.; Karnicka, K.; Frackowiak, E.; Beguin, F.; Kuhn, A.; Delville, M. H.; Starobrzynska, B.; Ernst, A. *Electrochim. Acta* **2006**, *51*, 2373−2379.
(43) Kowalewska, B.; Skunik, M.; Karnicka, K.; Miecznikowski, K.; Chojak, M.; Ginalska, G.; Belcarz, A.; Kulesza, P. J. *Electrochim. Acta* **2008**, *53*, 2408−2415.
(44) Kowalewska, B.; Kulesza, P. J. *Electroanalysis* **2009**, *21*, 351−359.
(45) Santiago, M. B.; Daniel, G. A.; David, A.; Casanas, B.; Hernandez, G.; Guadalupe, A. R.; Colon, J. L. *Electroanalysis* **2010**, *22*, 1097−1105.
(46) Xu, Z.; Gao, N.; Dong, S. J. *Talanta* **2006**, *68*, 753−758.
(47) Galus, Z. *Fundamentals of Electrochemical Analysis*, 2nd (revised) ed.; Ellis Horwood Limited: New York, 1994.